# The superfluid vortex cooler

# The superfluid vortex cooler

I. A. Tanaeva[a] and A. T. A. M. de Waele
*Department of Applied Physics, Eindhoven University of Technology, P.O. Box 513, NL-5600 MB Eindhoven, The Netherlands*

U. Lindemann, N. Jiang, and G. Thummes
*Institute of Applied Physics, University of Giessen, Heinrich-Buff-Ring 16, D-35392 Giessen, Germany*

(Received 18 February 2005; accepted 17 June 2005; published online 10 August 2005)

In this contribution a superfluid vortex cooler (SVC) is described. A SVC is a cooling device, the operation of which is based on the special properties of superfluid helium (He II). The SVC is small, simple, has no moving parts, and is gravity independent. It is capable of reaching temperatures as low as 0.65 K. First we have carried out a number of experiments, using a liquid-helium bath as a precooler for the SVC. Various geometries of the cooler components as well as the influence of the working pressure and the base temperature on the performance of the cooler have been investigated. Temperature below 1 K have been reached with a base temperature of 1.4 K. The next step has been combining the SVC with a pulse-tube refrigerator. In a preliminary experiment a lowest temperature of 1.19 K has been reached. Several ways to improve the system are suggested. © *2005 American Institute of Physics*. [DOI: 10.1063/1.2001730]

## I. INTRODUCTION

An increased need of cryogenic temperatures in research and high technology has caused a rapid development of cryocoolers during the last decade. The development in the field of pulse-tube refrigeration has been fast and impressive. A lot of work has been done on making pulse-tube refrigerators (PTRs) efficient and reliable. In 2003 a lowest temperature of 1.27 K has been reached with a two-stage PTR.[1] This temperature is just above the limiting temperature for PTRs, which is about 1 K. However, by using a PTR as a precooling stage, the lowest temperature can be brought further down. In this research we have used a PTR as a precooler for a superfluid vortex cooler[2,3] (SVC). The superfluid vortex cooler is small, simple, and has no moving parts. Therefore, by combining a PTR with a SVC we obtain a compact, cryogen-free cryocooler, capable of reaching temperatures well below 1 K.

The working fluid in a SVC is He II. He II is helium below the λ line (2.17 K at the saturated vapor pressure). It can be considered as a combination of two components: the normal component, which behaves just like any other viscous fluid, and the superfluid component, which has zero viscosity and entropy. At saturated vapor pressures the SVC is capable of reaching temperatures as low as 0.75 K.[4,5] At pressures close to the melting pressure the temperature can be brought down to 0.65 K.[6]

The operation of a SVC is based on two effects: the fountain effect and the vortex cooling effect. The essence of the fountain effect is that superfluid helium tends to flow in the direction of high temperature and maintains a pressure difference over a channel. This pressure difference is called the fountain pressure and can reach values as high as 70 kPa.

The vortex cooling takes place, when superfluid helium flows from a superleak into a capillary with a supercritical velocity. A superleak is a tube, tightly filled with fine powder, so that only the superfluid component can flow through it, while the normal component is blocked by its viscosity. If superfluid helium flows through a capillary with supercritical velocity, quantum vortices are created.[7,8] These vortices interact with the normal component, dragging it along the direction of the superfluid flow. The resulting reduced concentration of the normal component $\rho_n$ corresponds with a reduction of the temperature.[3,9] Therefore, cooling takes place.

Combining the fountain and the vortex cooling effects, we have designed and built the SVC. The SVC is a closed-cycle cooler. To cause the internal flow circulation heating power has to be supplied to the fountain pump. This heat has to be removed by a cryocooler or by a helium bath. In the case of a cryocooler the heat, supplied to the SVC, increases the precooling temperature, which has a negative effect on the coldest temperature of the SVC. If a liquid-helium bath is used, the precooling temperature can be fixed.

In the first set of experiments the SVC has been precooled by pumped liquid helium to temperatures between 1.2 and 1.7 K. First we have optimized the SVC for the lowest temperature. Later on we concentrated on reducing the input heating power. In the final set of experiments we have used a two-stage PTR as a precooler for the SVC. The results of the experiments are described in this contribution.

## II. CONCEPTUAL DESIGN OF THE SUPERFLUID VORTEX COOLER

### A. Operation principle of the SVC

The schematic diagram of the SVC is shown in Fig. 1. It consists of a main heat exchanger, a fountain part (superleak $S_1$, fountain heat exchanger $H_1$, and capillary $C_1$), and a vortex part (superleak $S_2$, vortex heat exchanger $H_2$, and capillary $C_2$). The main heat exchanger is attached to a precooling

[a]Author to whom correspondence should be addressed; FAX: +31-40-2438272; electronic mail: i.a.tanaeva@tue.nl

 

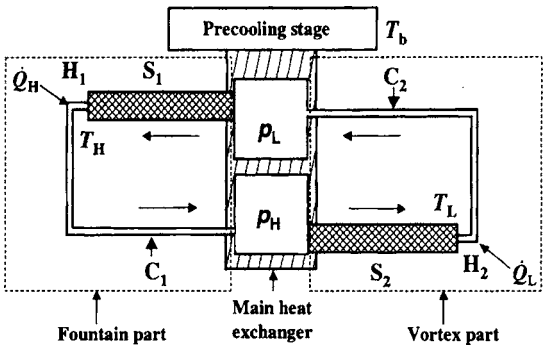


FIG. 1. Schematic diagram of the superfluid vortex cooler.

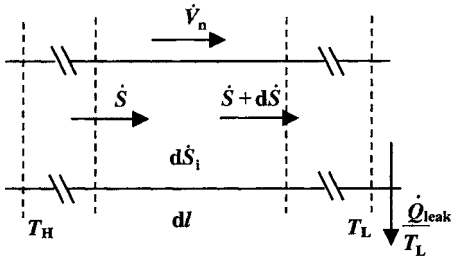


FIG. 2. Entropy, produced by a flow of normal helium in a channel. Normal helium flows from a high temperature and a high pressure to a low temperature and a low pressure. A certain amount of entropy is produced in the channel. Heat is removed at the low temperature $T_L$.

stage at a temperature $T_b$. At the beginning all parts of the system have a temperature $T_b$. By supplying heat to the heater $H_1$ we activate the fountain pump. The created pressure difference causes a flow of helium in the SVC from the low-pressure part of the main heat exchanger through $S_1$ and $C_1$. Helium arrives to the high-pressure part of the main heat exchanger with a temperature higher than $T_b$. It cools down in the heat exchanger and is then forced through $S_2$. Through $C_2$ the fluid returns to the low-pressure part of the main heat exchanger. The coldest point of the SVC is at the exit of $S_2$.

### B. Diameters of superleaks and capillaries

When designing the SVC, certain conditions have to be satisfied. The velocity of helium in the superleaks $v_s$ has to be lower than the superleak critical velocity $v_s^{\mathrm{cr}}$. The average velocity of helium in a superleak is given by

$$v_s = \frac{\dot{m}}{\rho_s(1-f)A_s}, \tag{1}$$

where $\dot{m}$ is a mass flow of the superfluid helium flowing through a superleak, $f$ is the filling factor, $\rho_s$ is the density of the superfluid helium, and $A_s = \pi d_s^2/4$ is the cross-sectional area of the superleak tube with the inner diameter $d_s$. According to the second law of thermodynamics the relation between the amount of heat $\dot{Q}_H$ supplied at one end of a superleak and the mass flow of helium in the direction of high temperature $T_H$ is

$$\dot{m} = \frac{\dot{Q}_H}{T_H s_H}, \tag{2}$$

where $s_H$ is the specific entropy of helium at temperature $T_H$. We require $v_s < v_s^{\mathrm{cr}}$. Therefore,

$$d_s^2 > \frac{4\dot{m}}{\rho_s \pi (1-f) v_s^{\mathrm{cr}}}. \tag{3}$$

In contrast with the superleak, the velocity of helium in the capillary $v_c$ should significantly exceed the critical velocity there $v_c^{\mathrm{cr}}$. In the capillary a quite complicated situation occurs. The velocity of the superfluid and the normal components can differ in magnitude and sign. At very high velocities, however, the coupling between the two components is so strong that the two velocities are equal; and He II flows as any normal fluid.[10] In this case we can write

$$v_c = \frac{\dot{m}}{\rho A_c}, \tag{4}$$

where $A_c = \pi d_c^2/4$ is the cross-sectional area of the capillary with the inner diameter $d_c$. Requiring that $v_c \gg v_c^{\mathrm{cr}}$, we can write

$$d_c^2 \ll \frac{4\dot{m}}{\rho \pi v_c^{\mathrm{cr}}}. \tag{5}$$

It has been found empirically[11] that the critical velocity is fairly temperature independent and varies with the fourth root of the channel diameter $d$ according to

$$v^{\mathrm{cr}} = \frac{C}{d^{1/4}}, \tag{6}$$

where $C \approx 1\ \mathrm{cm}^{5/4}\ \mathrm{s}^{-1}$. Equation (6) is valid for $d$, ranging from a few angstroms up to a few centimeters. The critical velocity of helium in superleaks, filled with jeweler's rouge powder, is typically 14–20 cm/s. For capillaries with diameters of a few tenths of a millimeters it is in the range of 2–5 cm/s.

### C. Losses in the SVC

Now we will discuss losses in the cooler, such as heat transport via the flow of normal helium, and dissipation in the capillaries. Using stainless steel as the material for capillaries and for the superleaks containers results in very small heat flow due to heat conduction, which can be neglected in any case.

#### *1. Imperfect superleaks*

Ideally the normal component cannot pass the superleak. However, in practice a superleak is just a large flow resistance. The pressure difference across $S_2$ causes the normal component to flow through it, resulting in a heat load on the coldest point of the SVC. A section of the superleak is drawn in Fig. 2. The normal component volume flow $\dot{V}_n$ is in the direction of the low temperature $T_L$. Applying the second law of thermodynamics to the section of the channel in the steady state gives the following expression:

$$d\dot{S} = d\dot{S}_i. \tag{7}$$

The change of the entropy flow $d\dot{S}$ is equal to the entropy production $d\dot{S}_i$ in it. The entropy production rate is expressed as[12]

$$d\dot{S}_i = -\dot{V}_n \frac{dp}{T}. \tag{8}$$

With Eq. (8), Eq. (7) can be written as

$$\frac{d\dot{S}}{dT} = -\frac{\dot{V}_n}{T}\frac{dp}{dT}. \tag{9}$$

The chemical potential $\mu$ in the superleak is constant, since the velocity of helium in the superleak is lower than the local critical velocity. So in this case the change in the pressure is equal to the change in the fountain pressure[13]

$$\frac{dp}{dT} = \frac{dp_f}{dT} = \rho s, \tag{10}$$

where $s$ is the specific entropy. With Eq. (10), Eq. (9) becomes

$$\frac{d\dot{S}}{dT} = -\frac{\dot{S}}{T}, \tag{11}$$

where

$$\dot{S} = \dot{V}_n \rho s. \tag{12}$$

Equation (11) leads to a constant value of $\dot{S}T$, which is equal to the heat load at the exit of the superleak

$$\dot{S}T = \dot{Q}_{\text{leak}}. \tag{13}$$

With Eqs. (12) and (13) we can write

$$\dot{V}_n \rho s T = \dot{Q}_{\text{leak}}. \tag{14}$$

The pressure gradient is given by

$$\frac{dp}{dl} = -\eta g_z \dot{V}_n, \tag{15}$$

where $g_z$ is a geometrical factor. With Eqs. (10) and (15) and assuming constant $\rho$, we obtain

$$\dot{Q}_{\text{leak}} = \frac{\rho^2}{g_z L}\int_{T_L}^{T_H} \frac{s^2}{\eta} T dT. \tag{16}$$

Using He II data from van Sciver,[14] an empirical equation for $s$ can be obtained as

$$s = s_0 T^{\alpha}, \tag{17}$$

where $s_0$ and $\alpha$ are given in Table I. The viscosity of helium below the lambda line is not constant,[15] but the temperature dependence of the viscosity has a rather flat plateau between 1.3 and 2 K. Therefore, in our calculations, we consider it to be constant and equal to $1.5 \times 10^{-6}$ Pa$\times s$.

Knowing $\dot{Q}_{\text{leak}}$ gives the heat leak due to the normal flow in the superleak. We will use this result later on to estimate the heat load on the coldest point of the SVC.

TABLE I. Empirical parameters $s_0$ and $\alpha$.

| $p$ (bar) | $s_0$ [J/(kg K$^{\alpha+1}$)] | $\alpha$ |
|---|---|---|
| SVP | 17.5 | 5.84 |
| 1 | 17.5 | 5.85 |
| 5 | 17.5 | 5.98 |
| 10 | 20.4 | 5.86 |
| 15 | 23.5 | 5.85 |
| 20 | 35.72 | 5.32 |

### 2. Energy balance in the capillaries

We consider uniform turbulent mass flow in the capillaries with a velocity significantly higher than the critical velocity of helium in a capillary. The energy transport by the vortices is neglected. Therefore, we can write the energy conservation law as

$$\frac{d}{dl}(\dot{m}h + \dot{Q}_{\text{He}}) = 0. \tag{18}$$

In Eq. (18) the specific enthalpy flow $h$ is a function of temperature and pressure according to the following thermodynamic relations:

$$\left(\frac{\partial h}{\partial T}\right)_P = c_p, \tag{19}$$

and

$$\left(\frac{\partial h}{\partial p}\right)_T = \frac{1}{\rho}. \tag{20}$$

The heat flow $\dot{Q}_{\text{He}}$ can be described by the Gorter-Mellink equation for the heat conduction in the flow of helium[16,17]

$$\dot{Q}_{\text{He}} = -A_c\left[\frac{1}{f_{\text{He II}}(T)}\frac{dT}{dl}\right]^{1/3}, \tag{21}$$

where

$$f_{\text{He II}}(T) = \frac{A\rho_n}{\rho_s^3 s^4 T^3}, \tag{22}$$

with $A$—the Gorter-Mellink parameter.[7,16,17] Combining Eqs. (18)–(21) gives

$$\dot{m}c_p\frac{dT}{dl} + \frac{\dot{m}}{\rho}\frac{dp}{dl} - A_c\frac{d}{dl}\left[\frac{1}{f_{\text{He II}}(T)}\frac{dT}{dl}\right]^{1/3} = 0. \tag{23}$$

Previous investigations[18,19] have shown that the friction factor in a flow of turbulent He II, $f_d$, is similar to the friction factor of classical fluids. Therefore, the pressure gradient in the capillary can be written as

$$\frac{dp}{dl} = -2f_d \rho v^2 \frac{1}{d_c}. \tag{24}$$

With Eq. (4), Eq. (24) becomes

$$\frac{dp}{dl} = -32\dot{m}^2 \frac{f_d}{\rho \pi^2 d_c^5}. \quad (25)$$

Simplifying Eq. (23) with Eq. (25), we can write

$$\dot{m} c_p \frac{dT}{dl} - 32\dot{m}^3 \frac{f_d}{\rho^2 \pi^2 d_c^5} - A_c \frac{d}{dl}\left[\frac{1}{f_{\mathrm{He\,II}}(T)} \frac{dT}{dl}\right]^{1/3} = 0. \quad (26)$$

This is the differential equation determining the temperature profile in the capillary. From this equation and with well-defined boundary conditions we can determine the heat flow in the capillaries. In Eq. (26) only $c_p$ and $f_{\mathrm{He\,II}}(T)$ are functions of temperature.[20] By bringing the equation in a dimensionless form and after some simple mathematics we obtain the following relation between the diameter of the capillary, the mass flow, and the characteristic temperature $T_0$

$$T_0^{4.7} = \frac{T_\lambda^{4.7}}{2} \frac{f_d \pi s_\lambda^4}{c_{p0}^4 A_\lambda} \frac{d_c}{\dot{m}}, \quad (27)$$

where $T_\lambda$ and $A_\lambda$ are the temperature and the Gorter-Mellink parameter at the λ point. From Eq. (27) it can be seen that $T_0$ is rather weak function of the capillary diameter. Nevertheless, keeping the same mass flow and decreasing the capillary diameter should decrease the minimum temperature, which is proportional to $T_0$. A typical value of $T_0$ for our SVC is 0.1 K.

Equation (26) can also be used to define the characteristic length of the vortex capillary $l_0$ as

$$l_0 = \left(\frac{\pi d_c^2}{4}\right)^3 \frac{\rho^2 s_\lambda^2 T_0}{A_\lambda} \left(\frac{1}{\dot{m} c_{p0}}\right)^3. \quad (28)$$

A typical value of $l_0$ for our SVC is in the order of a few microns.

## III. THE SUPERFLUID VORTEX COOLER, PRECOOLED BY A LIQUID-HELIUM BATH

### A. Experimental setup

A photograph of the SVC is represented in Fig. 3. All heat exchangers are copper blocks with channels inside. The capillaries are made of stainless steel. The superleaks are German silver tubes, filled with jeweler's rouge powder with a particle size of approximately 0.7 $\mu$m (for typical dimensions of the SVC components see Table II).

The SVC is placed in a vacuum chamber, which is pumped down to $10^{-4}$ Pa while the system is at room temperature. The vacuum chamber is immersed in liquid helium. The temperature of the liquid-helium bath is lowered by pumping. The main heat exchanger of the SVC contains a little volume with a channel of a few millimeters in diameter to the helium bath. Due to the very large thermal conduction of superfluid $^4$He, the helium in the volume has the same temperature as the bath. In this way the precooling of the SVC takes place. The SVC is connected to a helium supply at room temperature by two filling capillaries. Therefore, it is easy to vary the average pressure in the SVC. The filling capillaries extend from room temperature down to the SVC through the helium bath. The temperature is measured at the main heat exchanger $T_b$ at the fountain heat exchanger $T_H$ and at the vortex heat exchanger $T_L$. The thermometers at the fountain and the vortex heat exchangers are carbon ceramic and are calibrated down to 0.5 K. For measurements of $T_b$ a diode thermometer is used. The heaters are made of 50-$\mu$m manganine wire wound around copper holders, which are then soldered on the fountain and the vortex heat exchangers.

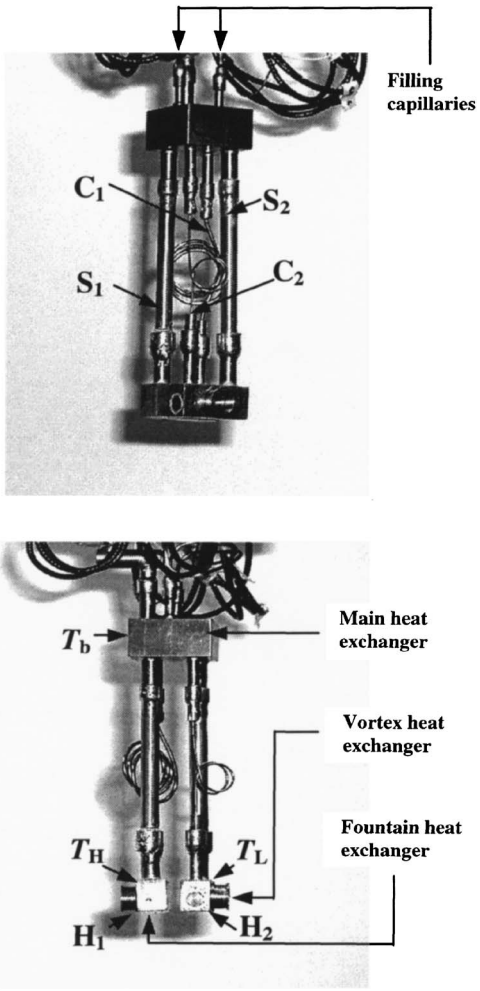


FIG. 3. The superfluid vortex cooler (for details see Fig. 2). The distance between the main heat exchanger and the fountain/vortex heat exchangers is about 6 cm.

### B. Results

In total 12 series of measurements (runs) have been made with the setup. The dimensions of the main components of the SVC, the lowest temperatures, reached in each run (excluding the trial runs 1 and 2), and the pressures, at which the lowest temperatures have been reached, are listed in Table II.

In run 3 we reached the lowest temperature of 0.88 K with an input heating power of 31.6 mW, a base temperature of 1.43 K (see Fig. 4), and a pressure of 9.8 bars. After run 3 we concentrated on reaching temperatures below 1 K with an input heating power as small as possible. The basic idea was to reduce the diameters of the superleaks and the capillaries so that the same velocities could be reached with less mass flow.

TABLE II. The dimensions of the main components of the SVC, the lowest temperature for each run, and the pressure, at which the lowest temperature is reached ( * the number in parentheses means the length of the filled part of a superleak). Sizes are in millimeters.

| | $S_1$ | | $C_1$ | | $S_2$ | | $C_2$ | | | |
|---|---|---|---|---|---|---|---|---|---|---|
| Run | $d_{S1}$ | $L^*_{S1}$ | $d_{C1}$ | $L_{C1}$ | $d_{S2}$ | $L^*_{S2}$ | $d_{C2}$ | $L_{C2}$ | $T_L$ (K) | $p$ (bar) |
| 3 | 2.5 | 46 (26) | 0.3 | 145 | 3.5 | 46 (26) | 0.7 | 281 | 0.883 | 9.8 |
| 4 | 3.5 | 46 (26) | 0.7 | 281 | 2.5 | 46 (26) | 0.3 | 145 | 0.932 | 10.0 |
| 7 | 3.5 | 46 (26) | 0.2 | 160 | 2.5 | 46 (26) | 0.2 | 80 | 0.909 | 10.0 |
| 8 | 1.5 | 40 (20) | 0.2 | 160 | 1.5 | 40 (20) | 0.2 | 80 | 0.986 | 10.8 |
| 9 | 1.5 | 40 (20) | 0.1 | 160 | 1.5 | 40 (20) | 0.1 | 80 | 1.025 | 10.6 |
| 10 | 1.5 | 40 (20) | 0.1 | 40 | 1.5 | 40 (20) | 0.1 | 80 | 1.056 | 10.7 |
| 11 | 3.5 | 46 (26) | 0.1 | 40 | 2.5 | 46 (26) | 0.1 | 80 | 1.083 | 10.4 |
| 12 | 3.5 | 46 (26) | 0.2 | 160 | 2.5 | 46 (26) | 0.2 | 80 | 0.944 | 13.7 |

Figure 4 shows two $\dot{Q}_H - T$ dependences, illustrating the influence of the diameter of the vortex capillary $d_{C2}$ on the performance of the SVC. Each set of measurements results in three curves. The lower curve is the temperature of the vortex heat exchanger ($T_L$), the middle curve is the base temperature ($T_b$), and the upper curve is the temperature of the fountain heat exchanger ($T_H$). At $\dot{Q}_H=0$ all parts of the SVC are at the base temperature. When heat is supplied to the fountain part, $T_H$ increases, and $T_L$ goes down, while $T_b$ remains almost constant. To reach 1 K with $d_{C2}=0.7$ mm one needs 18 mW, while with $d_{C2}=0.2$ mm only 3.5 mW of input heating power is needed to reach 1 K. This can be explained by the fact that the critical velocity is achieved at less mass flow in a capillary with a smaller diameter [see Eq. (7)]. Therefore, less heat input is needed to activate the cooling process.

Figures 5–7 represent $T_L$ as functions of $\dot{Q}_H$ for different dimensions of the main components of the SVC (runs 7–11 from Table II). The starting temperature in all measurements is 1.38 K and the pressure is around 10 bars. As it is seen from Fig. 5 the change of the superleak diameter (run 7 compared to run 8 and run 10 compared to run 11) does not affect the steepness of the curves at low $\dot{Q}_H$, but, as $\dot{Q}_H$ increases, the system with a larger superleak diameter reaches a lower temperature. The same mass flow, passing the superleak with a smaller diameter, causes higher velocity in it. Apparently this leads to an increase of the dissipation in the superleak. In run 10 the $\dot{Q}_H - T_L$ curve starts to level off at $\dot{Q}_H=1$ mW. Equations (2) and (3) imply that the superleak diameter should be larger than 0.7 mm. Since $d_s=1.5$ mm in run 10, this condition is satisfied. However, it seems that the diameter of the superleak should be heavily oversized in order that the SVC performs efficiently. This is also illustrated by the $\dot{Q}_H - T_L$ curve of run 11, in which $d_s$ has been increased up to 3.5 mm.

From run 8 to run 9 the diameters of both capillaries have been decreased by a factor of 2 (Fig. 6). In run 9 we see a steep cooldown at the beginning. However, the minimum temperature is higher than in run 8. From Eq. (27) it follows that, at constant mass flow, the minimum temperature should decrease with the capillary diameter. However, we observe an increase of the minimum temperature. This indicates a decrease of the mass flow. This may be the result of the increased entropy production at the entrance to the vortex capillary.

When decreasing the lengths of the capillaries from run 9 to run 10, we may have observed a certain critical value for the length (see Fig. 7). There is no difference in the perfor-

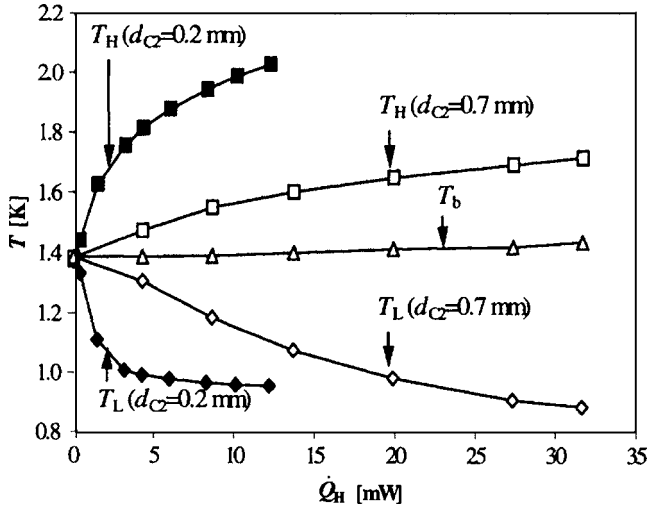


FIG. 4. The influence of the diameter of the vortex capillary $d_{C2}$ on the performance of the SVC. The average pressure in the SVC in both cases is 10 bars. Note that $T_b$ for $d_{C2}=0.2$ mm is not shown. For details see Table II.

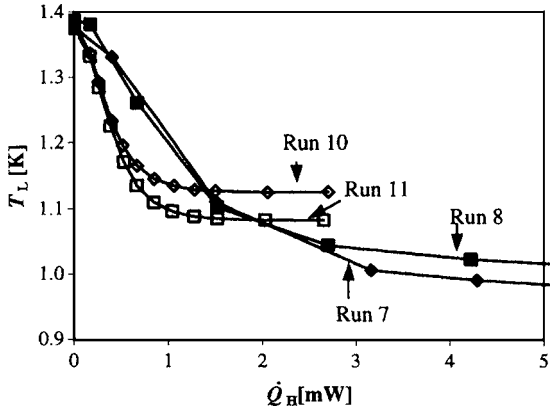


FIG. 5. The influence of the diameters of the superleaks on the performance of the SVC. The diameters of the superleaks have been decreased from run 7 to run 8. From run 10 to run 11 the diameters of the superleaks have been increased. For details see Table II.

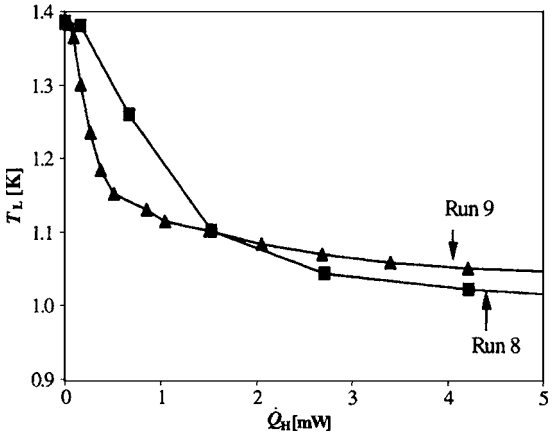


FIG. 6. $\dot{Q}_H - T_L$ dependences as affected by the reduction of the diameters of the capillaries from run 8 to run 9.

mance when the length of $C_2$ is decreased from 16 to 8 cm. However, when decreasing the length of $C_2$ further to 4 cm (run 10), the cooling curve starts to level off rather soon. The reason for this behavior has not been found yet. However, as the characteristic length of the vortex capillary is only a few microns (see Sec. II C 2), heat conduction in helium, as described by Eq. (26), cannot be the source of the observed phenomena.

Figure 8 demonstrates the influence of the pressure in the SVC on the performance of the cooler. For a given heating power $\dot{Q}_H$, $T_L$ is lower at higher pressures. As mentioned above, the cooling in the SVC results from the interactions between the superfluid vortices and excitations of the normal component: phonons and rotons. Rayfield and Reif[21] have shown that the rotons are much more scattered by vortices than by phonons. As the roton density increases with increasing pressure, this could explain the observation presented in Fig. 8.

We have also carried out several measurements with different base temperatures (see Fig. 9). Higher $T_b$ means that more heating power is needed to achieve the same $T_L$. In addition to that, the lowest temperature increases with the increase of $T_b$.

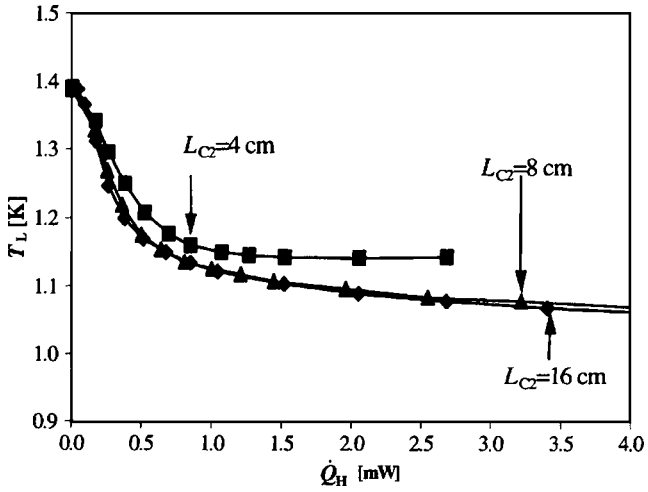


FIG. 7. $\dot{Q}_H - T_L$ dependences for three different lengths of $C_2$.

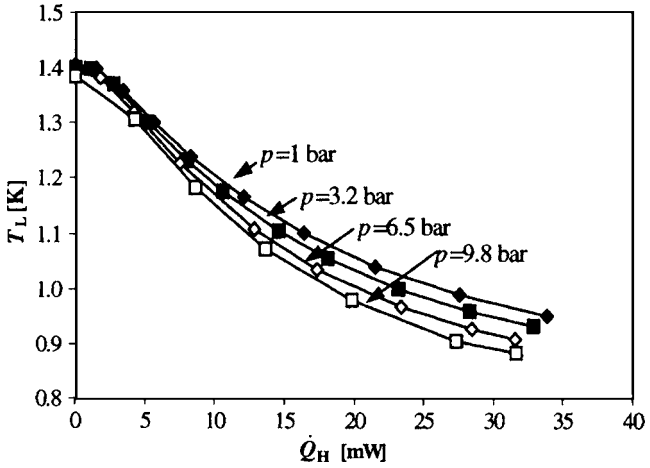


FIG. 8. The influence of the pressure in the SVC on the performance of the cooler. The geometry of the SVC for this experiment is given in Table II, run 3.

The cooling power of the SVC has been measured (see Fig. 10). At 1 K the cooling power is 130 $\mu$W with $\dot{Q}_H$ =8.75 mW (run 3) and 360 $\mu$W with $\dot{Q}_H$=31.6 mW (run 4). The coefficient of performance (COP) of a cooler is defined as

$$\mathrm{COP} = \frac{\dot{Q}_L}{\dot{Q}_H}. \tag{29}$$

The ideal COP of the SVC is[13]

$$\mathrm{COP}_{\mathrm{id}} = \frac{T_H - T_b}{T_H}\frac{T_L}{T_b - T_L}. \tag{30}$$

This can be used as a reference in further optimization of the SVC. It is interesting to see that Eq. (30) is the product of the efficiency of the Carnot engine, operating between $T_H$ and $T_b$, and the efficiency of the Carnot refrigerator, operating between $T_L$ and $T_b$. The experimental COP of our SVC at 1 K is 1.5%. It is equal to 7% of the ideal COP.

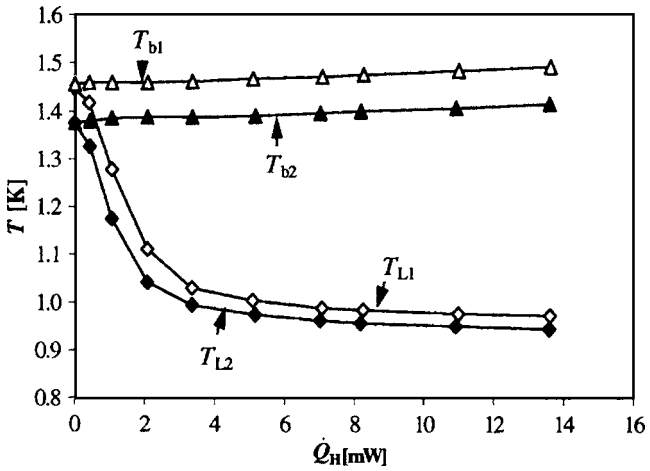


FIG. 9. The effect of the base temperature $T_b$ on the lowest temperature of the SVC $T_L$. The geometry of the SVC for this experiment is given in Table II, run 7.

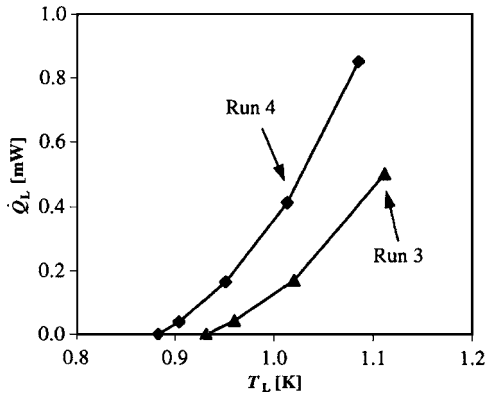


FIG. 10. Cooling power of the SVC at two different input heating powers and base temperatures. Run 3: $\dot{Q}_H$=8.75 mW, $T_b$=1.39 K. Run 4: $\dot{Q}_H$ =31.6 mW, $T_b$=1.43 K.

## IV. SUPERFLUID VORTEX COOLER, PRECOOLED BY A PULSE-TUBE REFRIGERATOR

### A. Experimental setup

The PTR, used as a precooler for the SVC, consists of two stages with separate gas circuits, as described in more detail elsewhere.[1] The $^4$He stage precools the $^3$He stage and the thermal shield down to 23 K. The $^3$He stage has a no-load temperature of 1.27 K and provides 8 mW of cooling power at 1.45 K.

The schematic diagram of the low-temperature part of the integrated system is shown in Fig. 11. The main heat exchanger of the SVC is clamped to the cold heat exchanger of the $^3$He stage. A thin layer of indium provides a good thermal contact between the PTR and the main heat exchanger of the SVC. For convenience the SVC is placed upside down, opposite to the experiments in the liquid-helium bath. A copper radiation shield (not shown in Fig. 11) is placed around the SVC and attached to the cold end of the second stage of the PTR. Several layers of superinsulation are wrapped around the heat shield for the thermal isolation.

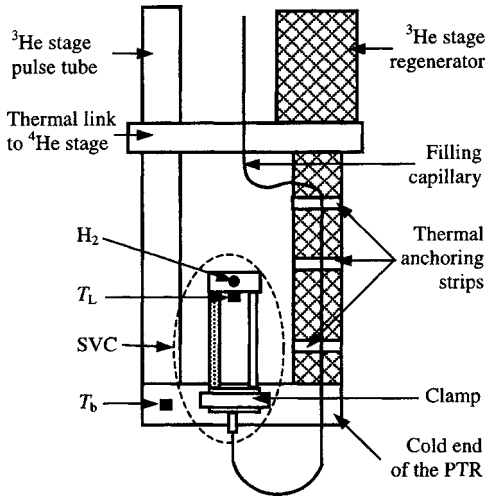


FIG. 11. Schematic diagram of the low-temperature part of the integrated PTR-SVC system. Only the vortex side of the SVC is shown in the figure. For details of the SVC—see Figs. 2 and 5.

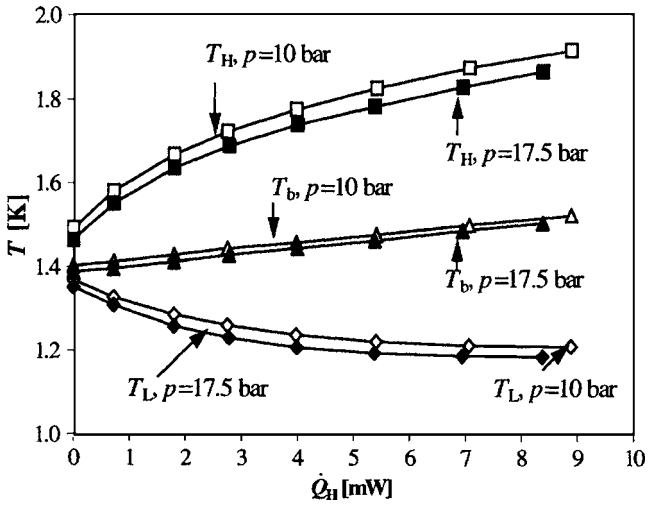


FIG. 12. Performance curves of the SVC, precooled by the PTR, at different pressures in the SVC. The lowest temperature of 1.19 K with $\dot{Q}_H$ =8.4 mW and $T_b$=1.5 K is reached.

The helium in the SVC is supplied via filling capillary extending from room temperature to one of the volumes of the main heat exchanger. The filling capillary is placed in vacuum and thermally anchored at a few places to the regenerator tube. The coldest anchoring point, at which the filling capillary is attached to the regenerator before entering the SVC, has approximately the lambda temperature. The main heat exchanger has the temperature $T_b$($\approx$1.4 K). Therefore, there is a fountain pressure difference of about 70 kPa in the lowest part of the filling capillary. This pressure difference drives a flow of normal helium from the coldest anchoring point to the main heat exchanger of the SVC. As a result there is a heat flow in the direction of the cold end of the PTR. To minimize this heat load, the last part of the filling capillary should be designed carefully. In our case the last 20 cm of the filling capillary has the diameter of 0.3 mm and is filled with a stainless-steel wire with a diameter of 0.27 mm. According to our estimation the heat leak through this capillary should be between 2 and 20 mW, depending on the shape of the gap between the walls of the filling capillary and the inserted stainless-steel wire.

### B. Results

In total 9 runs have been performed with the integrated system. The lowest no-load temperature of the PTR, before attaching the SVC, has been 1.27 K. With the SVC attached, the PTR reached a temperature of 1.48 K. After a renewed optimization the PTR reached a temperature of 1.39 K. The cooling power of the PTR at 1.39 K is around 5 mW,[1] which means that the heat leaks coming from the SVC, mainly from the filling capillary, amount to 5 mW.

Figure 12 demonstrates $\dot{Q}_H - T$ curves for two different average pressures in the SVC. The difference between $T_H$, $T_b$, and $T_L$ at zero applied heat load originates from a not yet identified heat load on the fountain heat exchanger that causes a slight cooling of the SVC, even before the external heat is applied. When applying heat to the fountain part of the SVC, both $T_H$ and $T_b$ increase. At the same time the

temperature of the vortex part, $T_L$, goes down. With 8.9 mW of input heating power and $T_b=1.52$ K a lowest temperature of 1.21 K has been reached (lines with open symbols in Fig. 12). The average pressure in the SVC in this case has been 10 bars. When the pressure in the SVC has been increased to 17.5 bars, the lowest temperature reduced to 1.19 K with 8.4 mW of input heat and $T_b=1.5$ K (lines with filled symbols in Fig. 12).

## V. CONCLUSIONS AND SUGGESTIONS

We have designed and built a superfluid vortex cooler. The cooler is rather simple, small, has no moving parts, works gravity independent, and requires little additional infrastructure. Several experiments have been carried out with a liquid-helium bath as a precooler for the SVC. A minimum temperature of 0.88 K with an input heating power of 31.6 mW has been achieved. The cooling power at 1 K is 360 $\mu$W.

After that the cooler has been modified, so that it could be used in combination with a PTR. The integration of the SVC with the PTR was successful and demonstrated very promising results. The integrated system reached a minimum temperature of 1.19 K with 8.37 mW of input heating power and with a pulse-tube cold head temperature of 1.5 K. This is a good starting point for optimizing the system to bring the temperature further down.

Hereby, we suggest two ways of improving the integrated system. As seen above, there is about 5 mW of heat, brought by the SVC to the PTR. Most of it comes from the filling capillary. In the present system the filling capillary enters the SVC at the main heat exchanger. If this filling capillary is connected to the fountain heat exchanger instead of the main heat exchanger, the parasitic heat load turns into a positive heat input, needed to activate the fountain pump. Another possibility would be to decrease the heat load to the cold end of the PTR by omitting the filling capillaries all together. In this case the necessary amount of helium must be filled into the vortex cooler at room temperature and at high pressures. Miniaturization of the SVC is another challenging field of research to be addressed in the future.

## ACKNOWLEDGMENTS

We acknowledge L. M. W. Penders, L. C. van Hout, J. J. G. M. van Amelsvoort, M. Bogers, J. Hermans, K. Verheyen, and P. Bruins for their contribution to the experimental part of the project, carried out in the Eindhoven University of Technology. We also thank F. Giebeler, Y. Kuecuekkaplan, M. Wagner, D. Hartung, L. Yang, and Z. Gan for their help during the part of the investigation, carried out at the University of Giessen.

[1] N. Jiang, U. Lindemann, F. Giebeler, and G. Thummes, Cryogenics **44**, 809 (2004).
[2] Not to be confused with the Ranque-Hilsch vortex tube, which is a cooling device near room temperature, described in the following article; C. Gao, K. J. Bosschaart, J. C. H. Zeegers, and A. T. A. M. de Waele, Cryogenics **45**, 173 (2005).
[3] P. Kapitza, Phys. Rev. **60**, 354 (1941).
[4] J. F. Olijhoek, J. K. Hoffer, H. van Beelen, R. de Bruyn Ouboter, and K. W. Taconis, Physica (Utrecht) **64**, 289 (1973).
[5] J. F. Olijhoek, H. van Beelen, R. de Bruyn Ouboter, and K. W. Taconis, Physica (Utrecht) **72**, 381 (1974).
[6] J. F. Olijhoek, H. van Beelen, R. de Bruyn Ouboter, K. W. Taconis, and W. Koops, Physica (Utrecht) **72**, 355 (1974).
[7] J. F. Olijhoek, Ph.D. thesis, Leiden University, 1973.
[8] F. A. Staas and A. P. Severijns, Cryogenics **9**, 422 (1969).
[9] I. M. Khalatnikov, *An Introduction to the Theory of Superfluidity* (Benjamin, New York, 1965).
[10] C. F. Barenghi, R. J. Donnelly, and W. F. Vinen, *Quantized Vortex Dynamics and Superfluid Turbulence* (Springer, Berlin, 2001).
[11] W. M. van Alphen, G. J. van Haasteren, R. de Bruyn Ouboter, and K. W. Taconis, Phys. Lett. **20**, 474 (1966).
[12] J. Wilks, *The Properties of Liquid and Solid Helium* (Clarendon, Oxford, 1967).
[13] I. Tanaeva, Ph.D. thesis, Eindhoven University of Technology, 2004.
[14] S. W. van Sciver, *Helium Cryogenics* (Plenum, New York, 1986).
[15] J. C. H. Zeegers, A. T. A. M. de Waele, and H. M. Gijsman, J. Low Temp. Phys. **84**, 37 (1991).
[16] C. J. Gorter and J. H. Mellink, Physica (Utrecht) **15**, 285 (1949).
[17] J. G. Weisend II, *Handbook of Cryogenic Engineering* (Taylor & Francis, Philadelphia, 1998).
[18] P. L. Walstrom, J. G. Weisend II, J. R. Maddocks, and S. W. van Sciver, Cryogenics **28**, 101 (1988).
[19] A. Hofmann, A. Khalil, and H. P. Kramer, Adv. Cryog. Eng. **33**, 471 (1988).
[20] A. Kashani and S. W. van Sciver, Adv. Cryog. Eng. **31**, 489 (1986).
[21] G. W. Rayfield and F. Reif, Phys. Rev. **136**, 1194 (1964).